

Histogram bin width selection for time-dependent Poisson processes

This article has been downloaded from IOPscience. Please scroll down to see the full text article.

2004 J. Phys. A: Math. Gen. 37 7255

(<http://iopscience.iop.org/0305-4470/37/29/006>)

View [the table of contents for this issue](#), or go to the [journal homepage](#) for more

Download details:

IP Address: 171.66.16.91

The article was downloaded on 02/06/2010 at 18:23

Please note that [terms and conditions apply](#).

Histogram bin width selection for time-dependent Poisson processes

Shinsuke Koyama and Shigeru Shinomoto

Department of Physics, Graduate School of Science, Kyoto University, Sakyo-ku,
Kyoto 606-8502, Japan

Received 18 March 2004, in final form 19 May 2004

Published 7 July 2004

Online at stacks.iop.org/JPhysA/37/7255

doi:10.1088/0305-4470/37/29/006

Abstract

In constructing a time histogram of the event sequences derived from a nonstationary point process, we wish to determine the bin width such that the mean squared error of the histogram from the underlying rate of occurrence is minimized. We find that the optimal bin widths obtained for a doubly stochastic Poisson process and a sinusoidally regulated Poisson process exhibit different scaling relations with respect to the number of sequences, time scale and amplitude of rate modulation, but both diverge under similar parametric conditions. This implies that under these conditions, no determination of the time-dependent rate can be made. We also apply the kernel method to these point processes, and find that the optimal kernels do not exhibit any critical phenomena, unlike the time histogram method.

PACS numbers: 02.50.Ey, 02.50.Tt, 87.19.La, 64.60.-i

1. Introduction

It is known that for a given neuron *in vivo*, the spike sequences generated in response to identical behavioural stimuli applied on separate occasions will not be identical. In such a situation that the spiking response contains some uncertainty, one must repeat the same trial a number of times to extract the actual signal of each neuron. The signal, or the message, is considered to underlie the rate of occurrence with which the spikes are evoked [1]. If the underlying rate is given *a priori* as a function of time, one would employ the maximum likelihood estimates to determine its parameters. In the general circumstance in which the underlying rate is not known, however, one should employ a nonparametric method for the inference of the underlying rate of occurrence. There have been proposed methods for filtering the rate of occurrence from a set of event sequences [2–7]. Among them, the most basic and easily applied method consists of constructing the time histogram for a series of events, or spikes. In fact, most rate evaluations for spike sequences recorded in neurophysiological

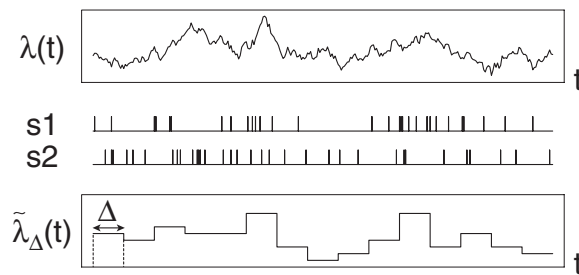


Figure 1. Sequences of point events, or spikes, (s1 and s2) derived from a time-dependent Poisson process with rate of occurrence $\lambda(t)$. From the set of spike sequences, a time histogram $\tilde{\lambda}_\Delta(t)$ of bin width Δ is constructed.

experiments are carried out using time histograms [8, 9]. In constructing a time histogram, one has to determine the bin width. A small bin width is necessary for capturing the details of the time dependence of the spike rate. If the bin width is too small, however, the time histogram fluctuates greatly, and we cannot discern the underlying rate of occurrence. In this paper, we determine the optimal bin width, with which the time histogram best approximates the underlying rate of occurrence.

Consider the situation that we observed n sequences of point events, or spikes, repeatedly derived from time-dependent Poisson processes characterized by the same time-dependent rate of occurrence, $\lambda(t)$ [10, 11]. With this set of data, one constructs a time histogram $\tilde{\lambda}_\Delta(t)$ to infer the underlying rate of occurrence $\lambda(t)$. The time histogram takes the form of a bar graph, consisting of bars of bin width Δ aligned along the time axis t (see figure 1). The height of each bar is proportional to the total number of spikes k that occurred within the time interval corresponding to this bin, divided by the product of the bin width Δ and the number of sequences n : $k/(n\Delta)$.

The goodness of the fit of the time histogram is evaluated by averaging the squared error from the underlying rate of occurrence over the total observation time T :

$$E_\Delta = \frac{1}{T} \int_0^T (\lambda(t) - \tilde{\lambda}_\Delta(t))^2 dt. \quad (1)$$

The total observation time T is assumed to be sufficiently large compared to Δ , so that the boundary effect can be ignored. The optimal bin width is defined as

$$\Delta^* \equiv \arg \min_{\Delta} E_\Delta. \quad (2)$$

In the following, we obtain the mean squared error analytically through averaging over all possible spike sequences generated with the rates of occurrence $\lambda(t)$ of a doubly stochastic Poisson process or a sinusoidally regulated Poisson process. We find that the optimal bin widths obtained for these point processes exhibit different scaling relations with respect to the number of sequences, time scale and amplitude of rate modulation, but both diverge under similar parametric conditions.

In addition to the time histogram method, we apply the kernel method to these point processes. It was found that the optimal kernels do not exhibit any critical phenomena, unlike the time histogram method.

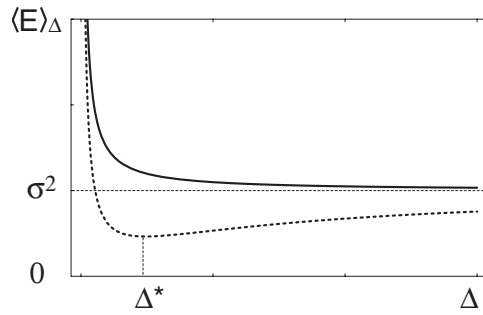


Figure 2. The mean squared error of the time histogram from the underlying rate of occurrence as a function of the bin width Δ . It either takes a minimum value at some finite Δ^* or decreases monotonically with Δ .

2. Bar graph time histograms

2.1. Doubly stochastic Poisson process

We first consider a doubly stochastic Poisson process, in which the rate of occurrence $\lambda(t)$ is a realization of the Ornstein–Uhlenbeck process,

$$\frac{d\lambda}{dt} = -\frac{\lambda - \mu}{\tau} + \sigma \sqrt{\frac{2}{\tau}} \xi(t) \tag{3}$$

where $\xi(t)$ is the Gaussian white noise with ensemble-averaged quantities $\langle \xi(t) \rangle = 0$ and $\langle \xi(t)\xi(t') \rangle = \delta(t - t')$. This process yields the fluctuating rate of occurrence $\lambda(t) = \mu + \sigma \eta(t)$, where μ is the mean rate, and $\eta(t)$ is a Gaussian random variable characterized by the ensemble average

$$\langle \eta(t) \rangle = 0 \quad \langle \eta(t)\eta(t') \rangle = e^{-|t-t'|/\tau}. \tag{4}$$

In this process, we stipulate that spikes are not generated when $\lambda(t) \leq 0$. Negative values of $\lambda(t)$ that may occur in the Ornstein–Uhlenbeck process result in errors in the analysis. The following analytical results are reliable for $\sigma^2\tau/\mu \ll 1$ [12].

The mean squared error E_Δ defined in (1) for a particular realization of the Ornstein–Uhlenbeck process, $\lambda(t)$, is expected to be self-averaging in the limit of a long observation time, $T \rightarrow \infty$, and in this case, E_Δ can be replaced with its average over Gaussian distributed ensembles of $\eta(t)$, denoted as $\langle E \rangle_\Delta$. This mean squared error is analytically obtained as

$$\langle E \rangle_\Delta = \sigma^2 + \frac{\mu}{n\Delta} - \frac{2\tau\sigma^2}{\Delta} + \frac{2\tau^2\sigma^2}{\Delta^2}(1 - e^{-\Delta/\tau}). \tag{5}$$

This quantity either takes its minimum value at some finite $\Delta = \Delta^*$ or decreases monotonically with Δ (see figure 2). The optimal bin width Δ^* is finite if

$$z \equiv n\sigma^2\tau/\mu > 1/2. \tag{6}$$

In other words, determination of the time-dependent rate cannot be made unless this condition (6) is met. The boundaries between regions in the parameter space in which different types of behaviour are exhibited are depicted in figure 3 for several values of n .

In the asymptotic limit, $z \gg 1$, the optimal bin width Δ^* , determined by $d\langle E \rangle_\Delta/d\Delta = 0$, obeys the scaling relation

$$\Delta^*/\tau \sim z^{-1/2}. \tag{7}$$

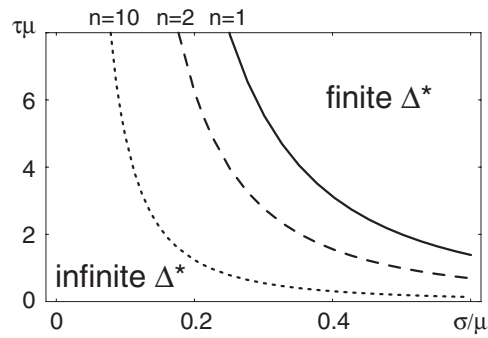


Figure 3. Boundaries between the parameter regions in which Δ^* is finite and infinite in the space of the (dimensionless) amplitude σ/μ and time scale $\tau\mu$ of rate modulation. These boundaries depend on the number of event sequences n .

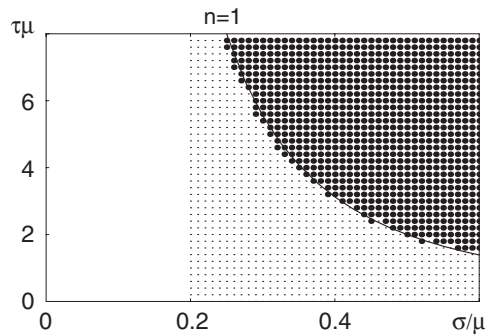


Figure 4. Results of numerical computation for Δ^* . Parameter values at which we obtain a finite value of Δ^* are indicated by filled circles, and those for which we obtain $\Delta^* = \infty$ are indicated by small dots. The analytical solution for the boundary in the case $n = 1$ ($\sigma^2\tau/\mu = 1/2$, depicted by a line) lies outside the range of validity for the analysis (i.e. that in which $\sigma^2\tau/\mu \ll 1$), but is nonetheless in fairly good agreement with the simulation results.

In this limit, the mean squared error is estimated as

$$\langle E \rangle_{\Delta^*} \sim \sqrt{4/3} \sigma^2 z^{-1/2}. \quad (8)$$

For small n , the boundary between regions of finite and infinite Δ^* , defined by (6), is beyond the range of validity for the analytical treatment. That is, the condition $\sigma^2\tau/\mu \ll 1$ is not satisfied. In order to see how the boundary is modified from (6) for $n = 1$, we performed a numerical simulation consisting of the following steps. First, we derived a sequence of spikes from a doubly stochastic Poisson process for a period of $T = 10^6$. Then, for each sequence, we constructed two time histograms with bin widths $\Delta_1 = 100\tau$ and $\Delta_2 = 1000\tau$, and then computed E_{Δ_1} and E_{Δ_2} , according to (1). If $E_{\Delta_1} > E_{\Delta_2}$, we regarded the optimal bin width Δ^* to be infinite, and otherwise finite. Figure 4 compares the boundaries obtained analytically and numerically. It is seen that they exhibit good agreement, even for $n = 1$.

2.2. Sinusoidally regulated Poisson process

We next consider a sinusoidally regulated Poisson process, in which the rate of occurrence $\lambda(t)$ is modulated by a smooth sinusoidal function,

$$\lambda(t) = \mu + \sigma \sin \frac{t}{\tau} \quad (9)$$

where μ , σ and τ are, respectively, the mean rate, the amplitude of modulation and the time scale of modulation. Here, we assume $\mu > |\sigma|$.

The mean squared error for this process is evaluated as

$$E_{\Delta} = \frac{\sigma^2}{2} + \frac{\mu}{n\Delta} - \frac{\tau^2\sigma^2}{\Delta^2} \lim_{T \rightarrow \infty} \frac{\Delta}{T} \sum_{j=1}^{T/\Delta} \Upsilon_j^2 \quad (10)$$

where

$$\Upsilon_j = \cos \frac{j\Delta}{\tau} - \cos \frac{(j-1)\Delta}{\tau}. \quad (11)$$

The optimal determination of the rate can be obtained with a bin width satisfying $m\Delta^* = 2\pi\tau$, with integer m . The condition under which the histogram exhibits nontrivial modulation, $m = 2, 3, \dots$, is given by

$$z \equiv n\sigma^2\tau/\mu > \pi/8. \quad (12)$$

Note that this condition is similar to that given in (6), derived for the doubly stochastic Poisson process.

In the asymptotic limit, $z \gg 1$, the optimal bin width obeys the scaling relation

$$\Delta^*/\tau \sim z^{-1/3}. \quad (13)$$

Note that this scaling exponent is different from that of the doubly stochastic Poisson process (7). In this limit, the mean squared error is estimated as

$$E_{\Delta^*} \sim \sigma^2 z^{-2/3}. \quad (14)$$

3. Line graph time histograms

If the simple bar graph time histogram is replaced with other kinds of functions, the goodness of the fit to the true rate of occurrence might be improved. In order to test this possibility, we replace the bar graph time histogram with the line graph (piecewise linear function), which is constructed by connecting the top-centres of adjacent bars of the original bar graph.

3.1. Doubly stochastic Poisson process

For the doubly stochastic Poisson process, the mean squared error is obtained as

$$\begin{aligned} \langle E \rangle_{\Delta} = & \sigma^2 + \frac{2\mu}{3n\Delta} + \frac{8\tau^3\sigma^2}{\Delta^3} - \frac{\tau^2\sigma^2}{\Delta^2} - \frac{5\tau\sigma^2}{3\Delta} - \frac{12\tau^3\sigma^2}{\Delta^3} e^{-\Delta/2\tau} + \frac{4\tau^3\sigma^2}{\Delta^3} e^{-3\Delta/2\tau} \\ & + \frac{2\tau^2\sigma^2}{3\Delta^2} e^{-\Delta/\tau} + \frac{\tau^2\sigma^2}{3\Delta^2} e^{-2\Delta/\tau}. \end{aligned} \quad (15)$$

In this case, the optimal bin width Δ^* is finite if

$$z > 2/5. \quad (16)$$

This condition is similar to those given in (6) and (12), although the numerical values differ.

In the asymptotic limit, $z \gg 1$, the optimal bin width obeys the scaling relation

$$\Delta^*/\tau \sim z^{-1/2} \quad (17)$$

which is the same as the scaling relation (7) obtained for the bar graph time histogram. In this limit, the mean squared error is estimated as

$$\langle E \rangle_{\Delta^*} \sim \sqrt{37/54} \sigma^2 z^{-1/2}. \quad (18)$$

This value of the mean squared error obtained with the line graph time histogram is smaller than that obtained with the bar graph time histogram (8), by the amount

$$(\sqrt{4/3} - \sqrt{37/54}) \sigma^2 z^{-1/2} \approx 0.33 \sigma^2 z^{-1/2}. \quad (19)$$

3.2. Sinusoidally regulated Poisson process

For the sinusoidally regulated Poisson process, the mean squared error is obtained as

$$\begin{aligned}
 E_{\Delta} = & \frac{\sigma^2}{2} + \frac{2\mu}{3n\Delta} + \frac{\tau^2\sigma^2}{\Delta^2} \lim_{T \rightarrow \infty} \frac{\Delta}{T} \sum_{j=1}^{T/\Delta} \left(\frac{1}{3}\Phi_j^2 + \frac{1}{3}\Phi_{j-1}^2 + \frac{1}{3}\Phi_j\Phi_{j-1} \right. \\
 & \left. - 2\Phi_{j-1}\Phi_{j-1/2} - 2\Phi_j \sin \frac{j\Delta}{\tau} + 2\Phi_{j-1} \sin \frac{j\Delta}{\tau} \right) \\
 & - \frac{2\tau^3\sigma^2}{\Delta^3} \lim_{T \rightarrow \infty} \frac{\Delta}{T} \sum_{j=1}^{T/\Delta} (\Phi_j \Upsilon_j - \Phi_{j-1} \Upsilon_j) \quad (20)
 \end{aligned}$$

where Υ_j is given in (11), and

$$\Phi_j = \sin \frac{(j+1/2)\Delta}{\tau} - \sin \frac{(j-1/2)\Delta}{\tau}. \quad (21)$$

The condition under which the histogram exhibits nontrivial modulation, $k\Delta^* = 2\pi\tau$ with $k = 2, 3, \dots$, is given by

$$z > \pi/(48/\pi - 4). \quad (22)$$

This condition is similar to those given in (6), (12) and (16), although the numerical values differ.

In the asymptotic limit, $z \gg 1$, the optimal bin width obeys the scaling relation

$$\Delta^*/\tau \sim z^{-1/5}. \quad (23)$$

The exponent, $-1/5$, of this scaling relation is different from the exponent, $-1/3$, of the scaling relation (13) obtained for the bar graph time histogram. In this limit, the mean squared error is estimated as

$$E_{\Delta^*} \sim \sigma^2 z^{-4/5}. \quad (24)$$

This mean squared error obtained with the line graph time histogram (24) is much smaller than that obtained with the bar graph time histogram (14).

4. Intuitive understanding of the scaling relations

The optimal bin widths obtained for the doubly stochastic Poisson process and the sinusoidally regulated Poisson process exhibit different scaling relations with respect to the number of sequences, time scale and amplitude of rate modulation. We now seek to obtain an intuitive understanding of these scaling relations.

Estimation error could arise from two kinds of causes: (i) statistical fluctuation due to the finite number of sampled data; and (ii) systematic error which arises by approximating continuous function with a discontinuous bar graph of a finite bin width.

The finite sample statistical fluctuation (i) is estimated as follows. The number of spikes that occur in each bin is approximately equal to $n\mu\Delta$. From the central limit theorem, we know that the typical size of the statistical fluctuation of the spike rate is approximately $\mu \times 1/\sqrt{n\mu\Delta} = \sqrt{\mu/(n\Delta)}$, which decreases with the bin width Δ . On the other hand, the systematic error (ii) increases with the bin width Δ . For a smooth rate function $\lambda(t)$, such as a sinusoidal function, the systematic error increases linearly with the bin width, in proportion to $\sigma\Delta/\tau$. The balance of the two kinds of errors, represented by the relation $\sqrt{\mu/(n\Delta)} \sim \sigma\Delta/\tau$, results in the scaling relation $\Delta^*/\tau \sim (n\sigma^2\tau/\mu)^{-1/3}$, which is in accordance with (13). The

mechanism for this scaling is the same as that for Scott's choice of the number of bars used to construct histograms [13].

The scaling relation is dependent on the smoothness of the probability modulation. In the case that the rate function fluctuates in a zigzag form, as when modulated by the Ornstein–Uhlenbeck process, the systematic error increases with $\sigma\sqrt{\Delta/\tau}$ for a short time interval. The balance of these two kinds of errors, i.e. the condition $\sqrt{\mu/(n\Delta)} \sim \sigma\sqrt{\Delta/\tau}$, results in the scaling relation $\Delta^*/\tau \sim (n\sigma^2\tau/\mu)^{-1/2}$, which is in accordance with (7).

In a practical application, we can make use of the knowledge of how to change (scale) the bin width with respect to the number of samples n . In the case that the underlying probability distribution is smooth, the bin width should be scaled in proportion to $n^{-1/3}$, while in the case that the underlying probability distribution takes the form of a greatly fluctuating zigzag, the bin width should be scaled in proportion to $n^{-1/2}$.

When the bar graph histogram is replaced by a line graph histogram, the optimal bin width obeys a different scaling relation, given by (23). It is also possible to obtain an intuitive understanding of this result. In approximating a smooth function with a piecewise linear function, the systematic error (ii) increases quadratically with the bin width as $\sigma(\Delta/\tau)^2$. The balance of this with the finite sample statistical fluctuation (i), that is, the condition $\sqrt{\mu/(n\Delta)} \sim \sigma(\Delta/\tau)^2$, results in the scaling relation $\Delta^*/\tau \sim (n\sigma^2\tau/\mu)^{-1/5}$, which is in accordance with (23). This argument can be extended to the spline interpolation of ℓ th order. In this case, we obtain a systematic error of order $\sigma(\Delta/\tau)^{(\ell+1)}$. The balance of two kinds of errors, represented by the relation $\sqrt{\mu/(n\Delta)} \sim \sigma(\Delta/\tau)^{(\ell+1)}$, results in the scaling relation $\Delta^*/\tau \sim (n\sigma^2\tau/\mu)^{-1/(2\ell+3)}$.

In the case that the rate function fluctuates in the form of a zigzag, as when modulated by the Ornstein–Uhlenbeck process, however, neither a piecewise linear function nor a higher-order spline interpolation method improves the systematic error qualitatively, because of the Brownian nature of the fluctuation, i.e. the systematic error increases with $\sigma\sqrt{\Delta/\tau}$.

We have also seen that the optimal bin widths obtained for the doubly stochastic Poisson process and the sinusoidally regulated Poisson process diverge under the similar conditions, namely $z = n\sigma^2\tau/\mu < O(1)$. For the following discussion, we are able to obtain an intuitive understanding of the mechanism responsible for the fact that in such a parameter range, the inference of the time-dependent spike rate is impossible.

As discussed above, the typical size of the statistical fluctuation of the spike rate in each bin is approximately $\sqrt{\mu/(n\Delta)}$. In order for the time histogram to reflect the underlying rate modulation, this statistical fluctuation should be smaller than the amplitude of the underlying rate modulation, σ . This condition yields the inequality $n\sigma^2\Delta/\mu > 1$. In addition, the bin width Δ should be smaller than the time scale of rate modulation, τ ; otherwise characterization of the time-dependent rate is impossible. This results in the final inequality, $n\sigma^2\tau/\mu = z > 1$. This inequality is similar to (6), (12), (16) and (22), differing only by numerical factors.

In a practical application, characteristics of the underlying rate of occurrence are generally not known *a priori*. In such a case, the optimal bin width may in principle be determined by using a cross-validation method: among the sequences derived from n repeated trials, take $n - m$ spike sequences to construct an empirical time histogram, and then apply this time histogram to the remaining m spike sequences to measure the goodness of the fit. However, it requires a huge amount of computation to maximize the goodness of the fit by repeating this procedure for different samples and bin widths. Our theoretical results for the two specific models do not exactly hold for general situations, but could give rough estimates of the reasonable bin width: as discussed in this section, the scaling relation of the optimal bin width obtained for each of two models holds among the same class of rate functions (smooth or

zigzag), and the parameter ranges in which the optimal bin width diverges are roughly the same in most cases.

5. Kernel method

The parameter range for which the optimal bin width Δ^* obtained with the line graph time histogram is finite is wider than that obtained with the bar graph time histogram. In fact, for a doubly stochastic Poisson process, the lower bound on $z = n\sigma^2\tau/\mu$ given in (16) for the line graph histogram, $2/5 = 0.4$, is smaller than that given in (6) for the bar graph histogram, $1/2 = 0.5$. For a sinusoidally regulated Poisson process, the lower bound on z given in (22) for the line graph histogram, $\pi/(48/\pi - 4) = 0.28$, is smaller than that given in (12) for the bar graph histogram, $\pi/8 = 0.39$. It is interesting to consider the possibility that the bin width Δ^* could remain finite for the entire parameter space if we employ better methods.

Consider again the situation in which we received a set of spike sequences derived from the (unknown) rate of occurrence $\lambda(t)$. In constructing a hypothetical rate of occurrence $\tilde{\lambda}(t)$ from the spiking data set, let us employ here the kernel method [8], in which a sequence of spikes is filtered with a kernel $K(t)$, as

$$\tilde{\lambda}(t) = \int_{-\infty}^{\infty} K(t')s(t-t') dt' \quad (25)$$

where $s(t)$ is the sequence of point events described as an array of the delta functions as

$$s(t) = \sum_{m=1}^n \sum_f \delta(t - t_f^{(m)}) \quad (26)$$

where $t_f^{(m)}$ is the time of the f th event, in the m th sequence. The squared error from the rate of occurrence, (1), could be minimized by choosing the kernel function as

$$K(t) = \frac{1}{2\pi} \int_{-\infty}^{\infty} \frac{\hat{Q}_{\lambda s}(-\omega)}{\hat{Q}_{ss}(\omega)} e^{-i\omega t} d\omega \quad (27)$$

where $\hat{Q}_{ss}(\omega)$ is the power spectrum of the event sequence, or equivalently, the Fourier transformation of the autocorrelation of the event sequence,

$$Q_{ss}(t) = \lim_{T \rightarrow \infty} \frac{1}{T} \int_0^T dt' s(t') s(t+t') \quad (28)$$

and $\hat{Q}_{\lambda s}(\omega)$ is the Fourier transformation of the correlation of the original rate and the event sequence,

$$Q_{\lambda s}(t) = \lim_{T \rightarrow \infty} \frac{1}{T} \int_0^T dt' \lambda(t') s(t+t'). \quad (29)$$

Those correlation functions and the consequent (optimal) kernel can be obtained analytically for the doubly stochastic Poisson process and sinusoidally regulated Poisson process, as follows.

5.1. Doubly stochastic Poisson process

The correlation functions $Q_{ss}(t)$ and $Q_{\lambda s}(t)$ for n sequences derived from the same rate of occurrence $\lambda(t)$ of a doubly stochastic Poisson process are obtained as

$$Q_{ss}(t) = n^2 \sigma^2 e^{-|t|/\tau} + n^2 \mu^2 + n\mu \delta(t) \quad (30)$$

and

$$Q_{\lambda_s}(t) = n\sigma^2 e^{-|t|/\tau} + n\mu^2. \quad (31)$$

Then the Fourier transformation of the optimal kernel (27) is given as

$$\hat{K}(\omega) = \frac{\hat{Q}_{\lambda_s}(-\omega)}{\hat{Q}_{s_s}(\omega)} = \frac{\frac{2n\tau\sigma^2}{\tau^2\omega^2+1} + 2\pi n\mu^2\delta(\omega)}{\frac{2n^2\tau\sigma^2}{\tau^2\omega^2+1} + 2\pi n^2\mu^2\delta(\omega) + n\mu}. \quad (32)$$

By representing the δ function as

$$\delta(\omega) = \lim_{\epsilon \rightarrow 0} \frac{\epsilon}{\pi(\omega^2 + \epsilon^2)} \quad (33)$$

the kernel is obtained as

$$K(t) = C_1 e^{-|t|/\tau_1} + \lim_{\epsilon \rightarrow 0} C_2(\epsilon) e^{-|t|/\tau_2(\epsilon)} \quad (34)$$

where

$$C_1 = \frac{\sigma^2}{\mu\sqrt{1+2n\tau\sigma^2/\mu}} \quad \tau_1 = \frac{\tau}{\sqrt{1+2n\tau\sigma^2/\mu}}$$

$$C_2(\epsilon) = \frac{\sqrt{\mu\epsilon}}{\sqrt{2n}(1+2n\tau\sigma^2/\mu)^{3/2}} \quad \tau_2(\epsilon) = \sqrt{\frac{1+2n\tau\sigma^2/\mu}{2n\mu\epsilon}}.$$

In this way the optimal kernel consists of two sub-kernels. It is notable that the time scale of the first sub-kernel, τ_1 , does not diverge, but is even shorter than the time scale of the original process, τ . However, the first sub-kernel contributes to the total integral $\int K(t) dt = 1/n$ only in a fraction of

$$\int_{-\infty}^{\infty} C_1 e^{-|t|/\tau_1} dt = \frac{2\tau\sigma^2/\mu}{1+2n\tau\sigma^2/\mu}. \quad (35)$$

The larger the rate modulation $\tau\sigma^2/\mu$, the larger the contribution of the first sub-kernel to the time integral, but it does not cover the total integral $\int K(t) dt = 1/n$. On one hand, the time constant of the second sub-kernel $\tau_2(\epsilon)$ diverges as $\epsilon \rightarrow 0$, and the second sub-kernel practically provides a window of an infinite width. This second sub-kernel covers a deficit of the time integral by

$$\int_{-\infty}^{\infty} C_2(\epsilon) e^{-|t|/\tau_2(\epsilon)} dt = \frac{1}{n(1+2n\tau\sigma^2/\mu)}. \quad (36)$$

In this way, the optimal kernel (34) does not exhibit any critical phenomena, unlike the bin width divergence in the time histogram method, but the kernel always contains a part, which is distributed infinitely in width (second sub-kernel here). The mean squared error is estimated as

$$\langle E \rangle \sim \sqrt{1/2}\sigma^2 z^{-1/2} \quad (37)$$

in the asymptotic limit $z = n\sigma^2\tau/\mu \gg 1$. The asymptotic exponent of the mean squared error obtained with the kernel method is identical to the exponent obtained with time histogram methods. The coefficient $\sqrt{1/2} = 0.707$ is smaller than not only the one obtained with the bar graph time histogram (8), $\sqrt{4/3} = 1.155$, but also the one obtained with the line graph time histogram (18), $\sqrt{37/54} = 0.828$.

5.2. Sinusoidally regulated Poisson process

In the same manner as above, $Q_{ss}(t)$ and $Q_{\lambda s}(t)$ for the sinusoidally regulated Poisson process are obtained as

$$Q_{ss}(t) = \frac{n^2\sigma^2}{2} \cos \frac{t}{\tau} + n^2\mu^2 + n\mu\delta(t) \quad (38)$$

and

$$Q_{\lambda s}(t) = \frac{n\sigma^2}{2} \cos \frac{t}{\tau} + n\mu^2. \quad (39)$$

Then the Fourier transformation of the optimal kernel (27) can be obtained as

$$\hat{K}(\omega) = \frac{\frac{\pi n\sigma^2}{2}\delta(\omega - 1/\tau) + \frac{\pi n\sigma^2}{2}\delta(\omega + 1/\tau) + 2\pi n\mu^2\delta(\omega)}{\frac{\pi n^2\sigma^2}{2}\delta(\omega - 1/\tau) + \frac{\pi n^2\sigma^2}{2}\delta(\omega + 1/\tau) + 2\pi n^2\mu^2\delta(\omega) + n\mu}. \quad (40)$$

By representing the δ function in the same form (33) as above, the kernel is obtained as

$$K(t) = \lim_{\epsilon \rightarrow 0} \left(C_1(\epsilon) e^{-|t|/\tau_1(\epsilon)} \cos \frac{t}{\tau} + C_2(\epsilon) e^{-|t|/\tau_2(\epsilon)} \right) \quad (41)$$

where

$$\begin{aligned} C_1(\epsilon) &= \sigma \sqrt{\frac{\epsilon}{2n\mu}} & \tau_1(\epsilon) &= \frac{1}{\sigma} \sqrt{\frac{2\mu}{n\epsilon}} \\ C_2(\epsilon) &= \sqrt{\frac{\mu\epsilon}{2n}} & \tau_2(\epsilon) &= \frac{1}{\sqrt{2n\mu\epsilon}}. \end{aligned}$$

In this way, the optimal kernel for the sinusoidally regulated Poisson process also consists of two sub-kernels. The first sub-kernel is periodic with the period identical to that of the original sinusoidal regulation. The kernel for this point process does not exhibit any critical phenomena either, but two sub-kernels are distributed infinitely in width. In this sinusoidally regulated case, only the second sub-kernel contributes to the total integral $\int K(t) dt = 1/n$. Amplitudes of both sub-kernels, $C_1(\epsilon)$ and $C_2(\epsilon)$, vanish in the limit of $\epsilon \rightarrow 0$ with the fixed ratio,

$$C_1(\epsilon)/C_2(\epsilon) \rightarrow \sigma/\mu. \quad (42)$$

Due to the perfect periodicity of the rate modulation in this special case, the underlying rate of occurrence is perfectly recovered.

6. Discussion

In the present study, we obtained the optimal bin widths in constructing time histograms for a doubly stochastic Poisson process and a sinusoidally regulated Poisson process, and found that they exhibit different scaling relations with respect to the number of sequences n , time scale τ , amplitude of rate modulation σ and the mean rate μ , but both diverge under similar parametric conditions, $n\sigma^2\tau/\mu < O(1)$. The divergence of the optimal bin width proved in this paper is not a special phenomenon for these two specific model processes, but is a rather general phenomenon that commonly holds for most time-dependent point processes. In experimental neuroscience, most rate evaluations for spike sequences have been carried out using time histograms. However, to our knowledge, there have been no serious discussions on the choice of the bin width. The divergence of the optimal bin width could be taken as a general warning that in estimating the underlying rate of occurrence with a finite bin width one might detect spurious signals.

We also examined the kernel method to seek for the better inference for the time-dependent rate of those two stochastic processes. It was found that the kernel does not exhibit any critical phenomena, unlike the time histogram method. In both point processes the optimal kernel consists of two sub-kernels, which are time dependent and constant. The time scale of a time-dependent sub-kernel always remains finite. Another sub-kernel is an (infinitesimal) constant with a window of an infinite width. In the limit of small amplitude of rate modulation σ , the first time-dependent sub-kernel vanishes. This is identical to the histogram method with the diverging bin width. The kernel method can provide some information even when the time histogram method cannot provide any information with respect to the underlying rate of occurrence.

Acknowledgments

This study is supported in part by grants-in-aid for scientific research to SS by the Ministry of Education, Culture, Sports, Science and Technology, Japan.

References

- [1] Rieke F *et al* 1996 *Spikes: Exploring the Neural Code* (Cambridge: MIT Press)
- [2] Snyder D L 1972 Filtering and detection for doubly stochastic Poisson processes *IEEE Trans. Inf. Theory* **18** 91
- [3] Boel R K and Beneš V E 1980 Recursive nonlinear estimation of a diffusion acting as the rate of an observed Poisson process *IEEE Trans. Inf. Theory* **26** 561
- [4] Manton J H *et al* 1999 Discrete time filters for doubly stochastic Poisson processes and other exponential noise models *Int. J. Adapt. Control Signal Process.* **13** 393
- [5] Ventura V *et al* 2002 Statistical analysis of temporal evolution in single-neuron firing rates *Biostatistics* **3** 1
- [6] Smith A C and Brown E N 2003 Estimating a state-space model from point process observations *Neural Comput.* **15** 965
- [7] Chi Z *et al* 2003 Pattern filtering for detection of neural activity, with examples from HVC activity during sleep zebra fishes *Neural Comput.* **15** 2307
- [8] Dayan P and Abbott L F 2001 *Theoretical Neuroscience* (Cambridge: MIT Press) pp 81–3
- [9] Kandel E R 2000 *Principles of Neural Science* 4th edn (New York: McGraw-Hill)
- [10] Cox D R and Lewis P A W 1966 *The Statistical Analysis of Series of Events* (New York: Wiley)
- [11] Tuckwell H C 1988 *Introduction to Theoretical Neurobiology* vol 2 (Cambridge: Cambridge University Press)
- [12] Shinomoto S and Tsubo Y 2001 Modeling spiking behaviour of neurons with time-dependent Poisson processes *Phys. Rev. E* **64** 041910
- [13] Scott D W 1992 *Multivariate Density Estimation* (New York: Wiley)